

Antibacterial, antifungal and antiviral activities of pyrimido [4,5-d]pyrimidine derivatives through computational approaches

Mahbub Alam ¹, Md. Eleas Kobir ², Ajoy Kumer ^{3*}, Unesco Chakma ⁴,
Parul Akter ⁵ and Md. Mosharef Hossain Bhuiyan ⁶

¹Inorganic Research Laboratory, Department of Chemistry, Jahangirnagar University Savar, Dhaka -1342, Bangladesh

²Department of Pharmacy, Atish Dipankar University of Science & Technology, Uttara, Dhaka-1230, Bangladesh

³Laboratory of Computational Research for Drug Design and Material Science, Department of Chemistry, European University of Bangladesh, Gabtoli, Dhaka-1216

⁴Department of Electrical and Electronics Engineering, European University of Bangladesh, Gabtoli, Dhaka-1216, Bangladesh

⁵Department of Chemistry, Mirzapur Cadet College, Mirzapur, Tangail – 1942, Bangladesh

⁶Department of Chemistry, University of Chittagong, Chittagong -4331, Bangladesh

(Received April 27, 2022; Revised June 18, 2022; Accepted July 02, 2022)

Abstract: Pyrimido[4,5-d]pyrimidine conveys antimicrobial activity against various micro pathogens having functionalized properties. As a result, this study has designed to illustrate the antibacterial, antifungal, and antiviral properties of pyrimido[4,5-d]pyrimidine. First of all, these structures have been optimized from the characterization of synthesis for calculating chemical descriptors by DFT. Next, the auto docking and target docking against 12 proteins, such as *Pseudomonas aeruginosa* (2Y0H), *Bacillus cereus* (1AH7), *Escherichia coli* (6DR3), *Shigella dysenteriae* (3FHH) *Salmonella typhi* (3FHU), *Aspergillus niger* (1ACZ), *Aspergillus flavus* (1XY3), *Rhizomucor miehei* (4WTP), *Candida auris* (6U8J), three proteins of SARS-CoV-2 (7T9J, 7T9L, and 7TB4) were performed for the determination of binding sites and binding affinity. One FDA approved drug (Ampicillin) has docked against 12 proteins while the *Bacillus cereus* (Bacteria), *Aspergillus flavus* (Fungus), and SARS-CoV-2, 7T9L (Omicron) are obtained the best binding affinity after docking. The most common residues are the PHE-66, ARG-176 and VAL-124 for *Bacillus cereus*, *Aspergillus flavus* and SARS-CoV-2, Omicron (7T9L), respectively, as they blocked the active sites by the ligands as inhibitors. It is revealed that this study contained both auto docking and target docking whereas the binding affinity of auto docking is that the binding affinity for auto docking is higher than target docking. Finally, among the nine compounds, three compounds show outstanding results against bacteria, fungus and virus. At last, molecular dynamics were performed to check the stability and validation of the docked complex and quantum calculations obtained the molecular properties, as well as ADMET, pharmacokinetics, Lipinski Rule and QSAR data.

Keywords: DFT; molecular dynamics; ADMET; Omicron; QSAR. ©2022 ACG Publication. All right reserved.

1. Introduction

Drug resistance is a common scenario nowadays in the human body. Among all the drugs, antibiotics, and antifungal are the most commonly resistant because of their abuse and maltreatment. At

* Corresponding author: E-Mail: kumarajoy.cu@gmail.com

Antimicrobial activities of pyrimido[4,5-d]pyrimidine derivatives

last, a small number of antiviral drugs are available in the market. Antibiotic resistance has increased to more than 2.8 million in the United States as a result, with over 35,000 people dying each year around the world.¹ Fungal infections frequently result in 50% or higher death rates, especially in the presence of antifungal resistance.² It is undoubtedly true that Omicron is a new variant of COVID-19, a viral disease, and has been considered the one of the largest worldwide epidemic. In addition, the omicron is the fastest spreading variant of COVID-19 and it multiplies 70 times faster than the delta variant of SARS-CoV-2.³ Because of the increasing number of drug for inhibitors and the availability of drugs, it is needed to develop a new drug. Due to fact of drug resistance, the natural product is the best solution as drugs so that the natural compound, pyrimido[4,5-d]pyrimidine derivatives are the one of the best considerable and acceptable solution for micro pathogens, because it has low resistance and toxicity in human body, as well as effective antibacterial activity⁴, antifungal activities⁵, potential pharmaceutical or biological activities,⁶ and potent antibacterial and biofilm inhibitors.⁷

In general, heterocyclic compounds are abundantly available and play a significant role in medication and the development of drugs and new bioactive compounds⁸. They also play a vital role in the physiology of all biological systems, and several of them are used clinically to treat a variety of disorders, whereas the pyrrolopyrimidines, pteridines, pyridopyrimidines, and purines are some of the examples of merged pyrimidines occurring in nature.⁹⁻¹¹ because of the vast range of medicinal actions, pyrimidine derivatives and heterocyclic annelated pyrimidines tend to pique attention, for instance antimicrobial,¹² anticancer,¹³ anti-inflammatory,¹⁴ antihistamine,¹⁵ antiviral,¹⁶ analgesic,¹⁷ and antifungal¹⁸ actions. Due to their structural closeness to purines, pyrimidopyrimidine derivatives have attracted a variety of interests in diverse pharmacological activities, such as anti-diabetic, anti-oxidant,¹⁹ and anti-tumor.²⁰ In the field of drug discovery, pyrimidopyrimidine derivatives are becoming a potential candidate for further investigation as potential drugs against the omicron variant as well as others.

Though, the nine pyrimido[4,5-d]pyrimidine derivatives had been synthesized and characterized at first. The synthesized crystals were performed against five pathogenic bacteria for *in vitro* tests where it could show a positive outcome, which is the cardinal motivation to continue their *in silico* study against various pathogens. As it had the characteristic and optimized chemical structures for nine pyrimido[4,5-d]pyrimidine derivatives, these structures were selected for the further analysis of computational study. Details of computational approaches, such as DFT, MD, chemical reactivity, drug likeness, protein ligand interaction, IR, UV, QSAR and different chemical descriptors are calculated. Then, the molecular docking study is the cardinal tool and fundamental point of this study to figure out the binding by ligand of the active site of proteins, and it is compared with the 03 FDA approved drugs named Ampicillin (Antibacterial), Fluconazole (Antifungal) and Molnupiravir (Antiviral) to obtain the proper acceptability of these derivatives. Finally, the best protein accounted for by auto docking in terms of binding affinity and molecular dynamics for each organism is selected for targeted docking where the active sites of proteins have been determined at first before going to this performance. However, this study transparently shows the comparative study of structure activity relationship, comparison of auto docking and targeted docking, *in vitro* study and its comparison with *in silico* study.

2. Experimental

2.1. Protein and Ligand Preparation

Five proteins of bacteria, four of fungus, and three proteins of omicron were selected from the RCSB protein data bank (<https://www.rcsb.org/>) by the justification of XRD data and its stable configuration of protein crystals. A total 12 proteins from the following organisms were downloaded in PDB format, and optimized these structure by PyMOL version 4.6 with the lower energy optimization in PDB format.²¹ On the other hand, the ligand of pyrimido[4,5-d]pyrimidine derivatives were geometrically optimized DMol3 code of material studio 08 setting the B3LYP with DNP basis set of functional of DFT (density functional theory).^{22,23}

2.2. Molecular Docking

Docking is a virtual screening method in molecular modeling used to predict ligand-protein interactions, and the ligand's binding orientation to target proteins. Moreover, it accurately predicts the binding affinity and activity of molecules.²⁴ Using PyRx by autodock tools, nine pyrimido[4,5-d]pyrimidine derivatives were used against twelve proteins for performing docking. In case of auto docking, the minimization energy and fixed grid box parameters were fixed by PyRx. In the case of targeted docking, the active sites of proteins (Table 1) are collected from their literature and calculated by the use of the Discovery Studio visualizer. Then, the targeted docking was performed by the same procedure as auto docking and recorded the binding affinity and files for calculating the ligand protein interactions.

Table 1. Active sites of best three proteins from bacteria, fungus and virus (omicron)

Protein Name	PDB ID	Active Sites
<i>Bacillus cereus</i>	1AH7	GLU-4, ASP-55, THR-65, PHE-66, TYR-79, ASP-122, HIS-128, HIS-142, GLU-146, and ASN-147
<i>Aspergillus flavus</i>	1XY3	TYR-30, CYS-103, ARG-105, TRP 106, ARG-128, ARG-176, ILE-177, TRP-208, TYR-257, PHE-258, and GLU-259
Cryo-EM structure of the SARS-CoV-2 of Omicron spike protein	7T9L	TRP-102, VAL-124, ILE-329, ALA-369, PHE-374, and SER-527

2.3. Protein Ligands Interaction

For the visualization of protein-ligand interaction, the Discovery Studio was used.²⁵ Identifying and analyzing the protein–ligand binding sites, which were obtained after docking as the docked complex by Discovery Studio, were acquired by 2D, 3D structures with type of bond and bond distance.²⁶

2.4. Pharmacokinetics and Toxicity (ADMET) Properties

Drug-likeness refers to how "drug-like" a material is regarding the factors, like bioavailability and Pharmacokinetics are the parameters to check the medications for the movement from side to side of the body. The drug likeness and pharmacokinetic properties of our ligands were determined using SwissADME (<http://www.swissadme.ch>).²⁷ On the other hand, the pkCSM (<http://biosig.unimelb.edu.au/pkcsml/>) is another website to calculated and evaluated ADMET (Absorption, Distribution, Metabolism, Excretion and Toxicity) properties of drug candidates.²⁸

2.5 Chemical Reactivity Prediction

The frontier molecular orbitals are the significance factor for the showing the chemical descriptors in term of HOMO, LUMO and HOMO-LUMO energy gap.²⁹ The following equation is used to calculate the chemical descriptors, such as global softness (S), electron affinity (A), ionization potential (I), electronegativity (X), global hardness (η), global electrophilicity index (H), and chemical potential (μ), of a drug candidate. The DFT theory was used for deducing the frontier molecular orbitals.^{30–32}

Antimicrobial activities of pyrimido[4,5-d]pyrimidine derivatives

$$E_{\text{gap}} = E_{\text{HOMO}} - E_{\text{LUMO}} \dots \dots \dots (1)$$

$$I = -E_{\text{HOMO}} \dots \dots \dots (2)$$

$$A = -E_{\text{LUMO}} \dots \dots \dots (3)$$

$$\mu = -(1+A)/2 \dots \dots \dots (4)$$

$$\eta = (1A)/2 \dots \dots \dots (5)$$

$$S = 1/\eta \dots \dots \dots (6)$$

$$\chi = (1+A)/2 \dots \dots \dots (7)$$

$$\omega = \mu^2/2\eta \dots \dots \dots (8)$$

2.6. Molecular Dynamics (MD)

The MD simulations of the top three binding affinity docked complex of pyrimido[4,5-d]pyrimidine derivatives for Bacteria, fungus, and omicron virus were run interactively with live view on a high configuration computer. To validate docking results, for the optimal ligand-protein interaction up to 100 ns for holo-form (drug-protein) using the AMBER14 force field MD simulation was used.³³ The total system is equilibrated with 0.9 percent NaCl at 298 K temperature in the presence of a water solvent. During the simulation, a cubic cell is propagated within 20 on each side of the process and periodic boundary circumstances, and the RMSD and RMSF were analyzed using the NAMD software after simulation.

2.7. Quantitative Structure-Activity Relationship

QSAR is characterized in computer-aided drug design by comparing it to drug-related eight descriptors obtained from ChemDes (<http://www.scbdd.com/chemdes/>), a free web-based platform for the calculation of molecular descriptors.³⁴ On the basis of mathematical and statistical correlations, quantitative structure-activity relationships (QSAR) were used to build connections between the physicochemical features of chemical compounds and their biological functions.^{35,36}

2.8. In Vitro Antibacterial Activity Evaluation

The antibacterial activities of unsaturated compounds were studied against five bacteria such as *Pseudomona aeruginosa*, *Escherichia coli*, *Bacillus cereus*, *Shigella dysenteriae* and *Salmonella typhi*. For the detection of antibacterial activities, nutrient agar (NA) was used as the basal medium for test bacteria. The composition of NA was beef extract (3g), peptone (5g), agar (15g), NaCl (0.5) and distilled water 1000mL. The inoculated slants were incubated at $(37 \pm 2)^{\circ}\text{C}$ in an incubator.

The ten (10) mL of distilled water were taken into a screw cap test Table for each organism and sterilized in an autoclave. From 48 hours old bacteria culture, one loop of culture was transferred to 10 mL of sterilized distilled water and mixed well. The bacteria suspension was added to the pour plate during the sensitivity test.

The antibacterial activity of the chemicals was detected by the disc diffusion method.³⁷ The paper disc of 4 mm in diameter and petri plates of 100 mm in diameter were used throughout the experiment while the culture plates were made with sterilized methods NA (45°C) and after solidification of agar medium^{38 39}. The test organisms (suspensions) were pressed uniformly over the plate with the sterilized glass rod separately. The paper discs after soaking with test chemicals at the rate of 20 $\mu\text{g}/\text{disc}$ were pleased at the center of the inoculated pour plate. A control plate was also maintained in each case with distilled water. The test was kept for 4 hours at a low temperature (4°C) and test chemicals diffused from disc to the surrounding medium by this time. The plates were then incubated at $(37 \pm 2)^{\circ}\text{C}$ for the growth of test organisms, and they were observed at 24-hour intervals for three days. The activity is expressed in terms of diameters of 24 hours intervals for three days. The activity is expressed in the terms of diameter of the zone of inhibition in mm. Each experiment was reported thrice.

3. Results and discussion

3.1. Chemistry and Optimized Structures of Study Compounds

The 5-aryl-7-thioxo-5,6,7,8-tetrahydropyrimido[4,5-d]pyrimidine-2,4-(1H,3H)-dione derivatives (PP1-PP9) have shown in Figure 1 which was synthesized by one-pot condensation reaction. Then, these compounds were characterized by UV, FTIR and NMR data, which confirmed their synthesis and molecular structure.⁴⁰ In order to determine molecular reactivity, chemical reactivity, and biological activity through the *in silico* study, the optimal and accurate molecular structure is the most significant factor. Material studio version 8.0 is one of most acceptable and considerable computational software, which has been used to optimize the nine molecular structures of pyrimido[4,5-d]pyrimidine derivatives, depicted in Figure 1.

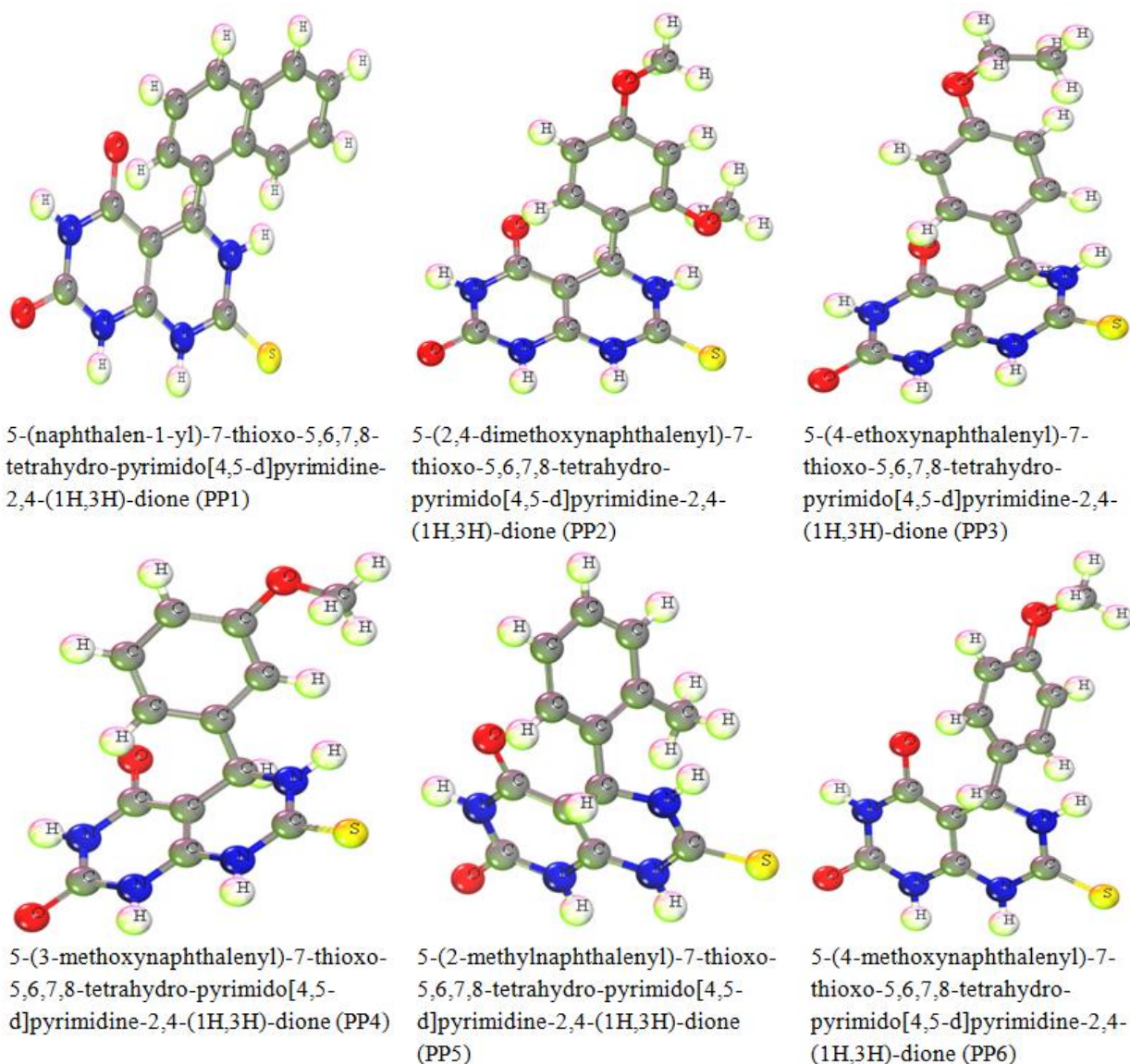


Figure 1. Optimized structure of ligands

Antimicrobial activities of pyrimido[4,5-d]pyrimidine derivatives

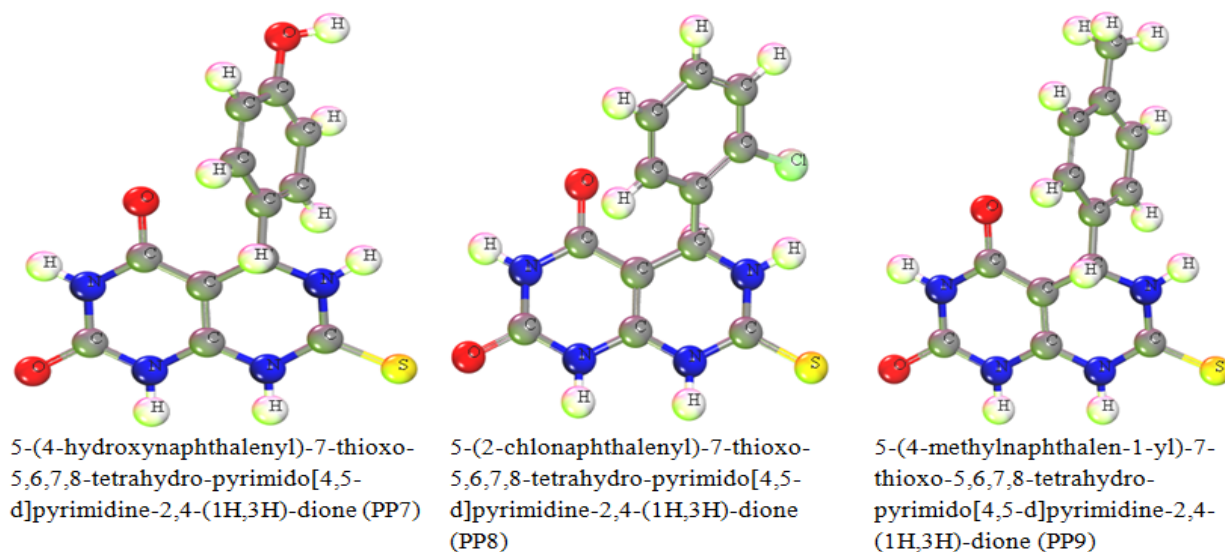


Figure 2. Optimized structure of ligands (continued)

3.2. Molecular Docking Analysis

Auto docking and targeted docking were performed by using nine pyrimido[4,5-d]pyrimidine derivatives against five proteins of bacteria named *Pseudomonas aeruginosa*, *Bacillus cereus*, *Escherichia coli*, *Shigella dysenteriae*, *Salmonella typhi* and PDB ID: 1AH7, 2YOH, 3FHH, 3FHU, and 6DR3, respectively. The four fungal proteins known as *Aspergillus niger*, *Aspergillus flavus*, *Rhizomucor miehei*, *Candida auris* and their PDB ID's are 1ACZ, 1XY3, 4WTP, and 6U8J, respectively. At last, the three proteins of the omicron variant for SARS-CoV-02, PDB ID: 7T9L, 7T9J, 7TB4 are taken for the docking procedure. After both targeted docking and auto docking, the result of binding affinity for auto docking shows more binding affinity towards the protein than for targeted docking. As a result, further experiments (*in vitro*, and molecular dynamics) were performed according to auto docking.

Table 2. Auto docking data against selected bacteria

Ligands Number	<i>Bacillus cereus</i>	<i>Pseudomonas aeruginosa</i>	<i>Shigella dysenteriae</i>	<i>Salmonella typhi</i>	<i>Escherichia coli</i>
PP1	-8.8	-7.8	-8.6	-7.9	-8.4
PP2	-7.9	-7.7	-7.7	-6.5	-6.6
PP3	-8.2	-8.0	-8.8	-6.6	-6.5
PP4	-8.8	-7.5	-8.6	-6.9	-6.6
PP5	-8.5	-7.3	-7.4	-6.6	-6.8
PP6	-7.8	-7.8	-8.4	-6.7	-6.9
PP7	-7.8	-8.3	-9.4	-6.9	-7.2
PP8	-8.5	-7.4	-8.7	-7.0	-6.8
PP9	-8.2	-8.3	-8.0	-6.7	-7.3
D1(Ampicillin)	-8.5	-7.4	-8.1	-6.3	-6.9

Despite the fact that the FDA-approved antibacterial drug ampicillin has the highest docking score with the protein 1AH7, as a result, 1AH7 has been considered for further research. The highest docking score for that following protein is -8.8 kcal/mol for PP1 against the *Bacillus cereus* and the lowest score at -7.8 kcal/mol for PP7 for *Bacillus cereus*. On the other hand, FDA approved drug ampicillin has the highest docking score is at -8.5 kcal/mol against *Bacillus cereus*. In addition, the PP1, PP4, PP5, and PP8 have

more or the same docking score than ampicillin(D1) represented in Table 2, and they are -8.8, -8.8, -8.5, and -8.5 kcal/mol, respectively.

In the case of Fungus, *Aspergillus flavus* (1XY3) a protein of fungus, which shows the highest docking score against FDA approved antifungal drug fluconazole and the docking score is at -7.4 kcal/mol, is considered for further study. The highest docking score is at -8.4 kcal/mol by the ligand, PP1 while the PP4, PP5, PP7, PP8, and PP9 ligands show more binding affinity than fluconazole standard drug shown in Table 3 with having the docking score at -7.6, -7.5, -7.6, -7.5, and -7.9 kcal/mol, respectively.

Table 3. Auto docking against Fungus

Ligands Number	<i>Aspergillus niger</i>	<i>Aspergillus flavus</i>	<i>Rhizomucor miehei</i>	<i>Candida auris</i>
PP1	-7.5	-8.4	-8.5	-8.1
PP2	-6.4	-7.4	-7.1	-6.8
PP3	-6.0	-7.0	-7.2	-7.1
PP4	-6.7	-7.6	-7.2	-7.2
PP5	-6.5	-7.5	-7.9	-7.0
PP6	-6.6	-7.3	-7.2	-7.0
PP7	-6.7	-7.6	-7.4	-7.3
PP8	-6.8	-7.5	-7.4	-7.0
PP9	-6.8	-7.9	-7.6	-7.6
D1 (Fluconazole)	-6.2	-7.4	-7.0	-7.1

Pyrimido[4,5-d]pyrimidine derivatives are also examined for three proteins of omicron, whereas the most commonly used anti-viral drug for omicron in Bangladesh is molnupiravir. The Molnupiravir shows the best binding affinity(-7.1 kcal/mol) with the SARS-CoV-2 for Omicron spike protein in complex with human ACE2 (7T9J) and -6.3 kcal/mol for the both 7T9L, and 7TB4 proteases. The most notable point that the PP1 shows the highest score of -8.4 kcal/mol against 7T9J while The binding score of PP4, PP5, PP8, and PP9 has more than molnupiravir at -7.2, -7.5, -7.5, and -7.4 kcal/mol, respectively. Table 4 shows the docking score against the omicron protein.

Table 4. Auto docking against Omicron

Ligands Number	Cryo-EM structure of SARS-CoV-2 Omicron spike protein in complex with human ACE2 (7T9J)	Cryo-EM structure of the SARS-CoV-2 Omicron spike protein (7T9L)	Cryo-EM structure of the spike of SARS-CoV-2 Omicron variant of concern(7TB4)
PP1	-8.4	-8.3	-8.4
PP2	-6.7	-6.3	-7.1
PP3	-6.5	-7.9	-7.0
PP4	-7.2	-6.5	-7.1
PP5	-7.5	-7.6	-7.0
PP6	-6.3	-6.9	-6.9
PP7	-7.0	-6.8	-7.2
PP8	-7.5	-7.5	-7.5
PP9	-7.4	-7.5	-7.5
D1 (Molnupiravir)	-7.1	-6.3	-6.3

Antimicrobial activities of pyrimido[4,5-d]pyrimidine derivatives

3.3. Target Docking of Bacteria

Active sites for the proteins of bacteria are calculated where the active sites for 1AH7 have ten, 2Y0H has twelve, 3FHH has nine, 3FHU has eight, and 6DR3 has eight, which were used for targeted docking.

The highest docking scores are at -5.2, -8.3, -9.2, -7.5, and -8.3 kcal/mol, respectively, in Table 5 for variable protein, which is much smaller than the auto docking. The main cause for the lower score in target docking is explained by the grid surface area. In the case of targeted docking, the grid box is limited, which can influence the lower docking score.

Table 5. Targeted docking against Bacteria

Ligands Number	<i>Bacillus cereus</i>	<i>Pseudomonas aeruginosa</i>	<i>Shigella dysenteriae</i>	<i>Salmonella typhi</i>	<i>Escherichia coli</i>
PP1	-5.2	-7.8	-8.6	-7.5	-8.3
PP2	-5.0	-7.0	-7.7	-6.8	-7.0
PP3	-3.8	-7.1	-8.8	-6.6	-6.8
PP4	-2.0	-7.3	-8.6	-7.1	-6.9
PP5	-2.8	-7.7	-7.4	-7.1	-7.0
PP6	-2.1	-7.9	-8.4	-6.8	-6.9
PP7	-2.6	-8.3	-9.2	-6.9	-6.7
PP8	-2.5	-7.3	-8.7	-7.0	-6.8
PP9	-2.7	-8.3	-8.0	-6.7	-7.3

3.4. Target Docking of Fungus

Active sites for the fungal protein of 1ACZ has 09, 1XY3 have 11, 4WTP has 11, and 6U8J has 13 and their highest docking score is at -6.9, -8.3, -8.2, and -7.5 kcal/mol respectively. Table 6 below shows the binding affinity of targeted docking. From Table 6, it is found that the binding affinity of *Aspergillus niger* is lower than that of *Aspergillus flavus*, *Rhizomucor miehei* and *Candida auris* pathogens. In all cases, the binding affinity for the *Aspergillus flavus* pathogen against all other pathogens where the PP1 ligand conveys the higher value, and it is decreased with the irregular fashion of the carbon chain.

Table 6. Targeted docking against Fungus

Ligands Number	<i>Aspergillus niger</i>	<i>Aspergillus flavus</i>	<i>Rhizomucor miehei</i>	<i>Candida auris</i>
PP1	-6.9	-8.3	-8.2	-7.5
PP2	-5.7	-7.4	-7.0	-6.8
PP3	-5.9	-7.5	-7.2	-7.1
PP4	-6.2	-7.4	-7.5	-7.1
PP5	-6.4	-7.6	-7.5	-6.7
PP6	-6.1	-7.3	-7.2	-6.8
PP7	-7.0	-7.6	-7.4	-6.9
PP8	-6.8	-7.4	-7.7	-7.1
PP9	-6.5	-7.7	-7.6	-7.2

3.5. Target Docking of Fungus

At last, the omicron protease has the following active sites; 7T9L has 06, 7T9J has 06, and 7TB4 has 07 active binding regions. The highest binding affinities are at -7.4, -7.4 and -6.8 kcal/mol for ligand, PP1 against three proteases, respectively. Table 7 below shows the targeted docking score against the omicron protein. After performing docking against a selected protein residue, the docking score is lower than the auto docking. The target docking result is always lower with increasing the length of chains.

Table 7. Targeted docking against Omicron

Ligands Number	Cryo-EM structure of SARS-CoV-2 Omicron spike protein in complex with human ACE2	Cryo-EM structure of the SARS-CoV-2 Omicron spike protein	Cryo-EM structure of the spike of SARS-CoV-2 Omicron variant of concern
PP1	-7.4	-7.4	-6.8
PP2	-6.2	-6.2	-6.1
PP3	-6.1	-6.0	-6.0
PP4	-6.5	-6.2	-6.1
PP5	-6.4	-6.7	-6.3
PP6	-6.8	-6.8	-5.8
PP7	-6.8	-6.8	-6.2
PP8	-6.2	-6.3	-6.2
PP9	-7.0	-6.9	-6.3

3.6. Comparative Study between Selective Docking and Auto Docking

After a comparison between target docking and auto docking, it is lucidly clear that auto docking shows more binding affinity than target docking. There are some reasons behind this lower result for target docking. For instance, lower grid and constricted opportunity for binding ability between protein and ligand can be considered as reasons behind this. It can be a new approach for target and auto docking although most of the compounds show anti-bacterial, antifungal and antiviral (Omicron) properties throughout the docking study. The highest docking scores for bacteria are at -9.2 and -9.4 kcal/mol for target docking and auto docking. The FDA approved antibiotic drug (ampicillin) has the highest potentiality against *Bacillus cereus* by auto docking, but in regards to target docking, it shows the lowest docking score, whereas the docking score is less than -6.00 kcal/mol. Next, the docking scores of fungus protein (1XY3), it is recorded at -8.3 and -8.5 kcal/mol for targeted and auto docking, respectively. Finally, the highest auto docking score of omicron protein (7T9L) is at -8.4 kcal/mol which is also superior for omicron than the highest targeted docking score, at -7.4 kcal/mol. However, this study elaborates that auto docking is better than the site specific docking known as the targeted docking. Figure 2 (a, b, c) represents a comparative study between auto and target docking scores among three different pathogens. The bar graph clearly states the comparison of the binding affinity between auto docking and target docking where the binding energy of auto docking is higher than target docking. In Figure 2(a), the docking score of targeted docking is too low. The reason, in auto docking and targeted docking their binding sites are different, as well as the type of bond nature, even bond distance. For Figure 2(b), targeted docking of PP3 and PP5 is higher than auto docking and at last, for Figure 2(c), binding affinity for all ligands of auto docking is higher than targeted docking. From those Figures, it clarifies that auto docking score is higher than targeted docking.

Antimicrobial activities of pyrimido[4,5-d]pyrimidine derivatives

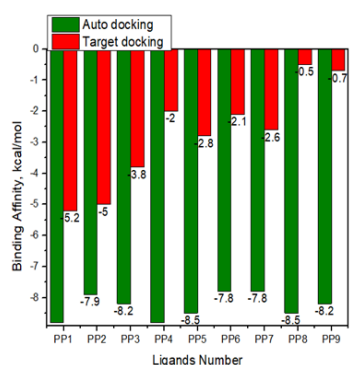


Figure 2 (a). Comparative study of auto and targeted docking of *Bacillus cereus*

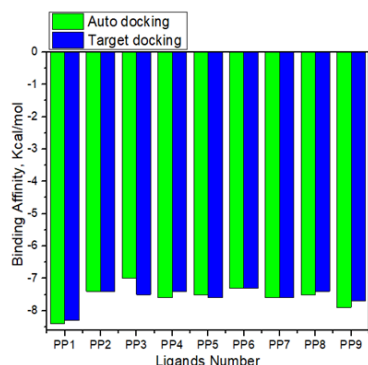


Figure 2 (b). Comparative study of auto and targeted docking of *Aspergillus flavus*

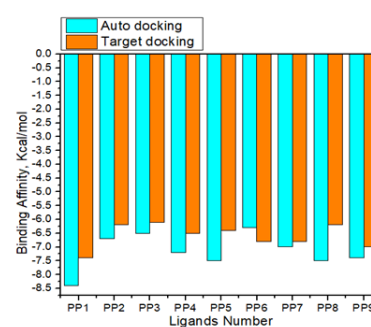
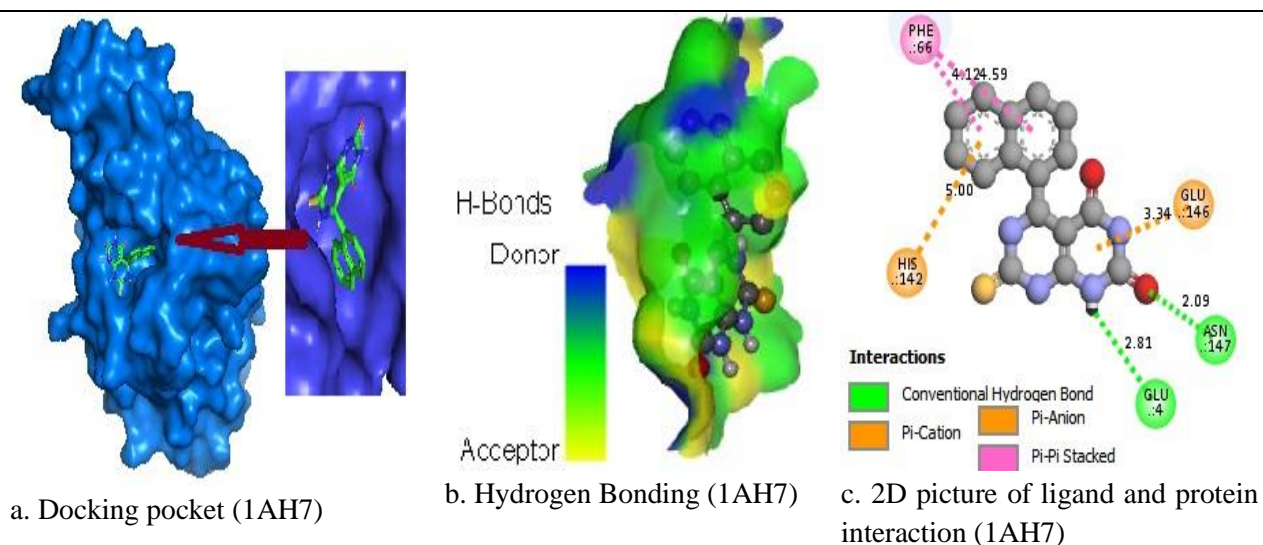


Figure 2 (c). Comparative study of auto and targeted docking of SARS-CoV-2 (Omicron)

3.7. Protein Ligands Interaction

Protein ligand interactions of nine pyrimido[4,5-d]pyrimidine derivatives against bacteria, fungus and omicron variants of COVID-19 are studied. Three proteins are taken among twelve proteins of three different organisms. These three proteins are taken based on their highest docking score against Ampicillin, Fluconazole and Molnupiravir. In this study, the highest residue of protein and the lowest bond distance were experimentally determined. The lowest bond distance mentioned compounds more affinity and strong binding towards protein. Conventional Hydrogen bonds and hydrophobic bonds are taken and other bonds are ignored.

For bacterial protein, 1AH7 (*Bacillus cereus*), the highest interacted protein residues are in GLU-146, PHE-66, and TRP-1 shown in Table S1. These are repeated 14, 13 and 7 times, respectively. The lowest bond distance is at 2.002 Å with the residue ASN-147 for the ligand PP5. Another four lowest bond distances are at 2.088 Å, 2.121 Å, 2.137 Å, and 2.142 Å with the residue ASN-147, TYR-79, THR-65, GLU-146, respectively in the ligands PP1, PP2, PP4 and PP9, respectively, depicted in Table 8. From this study, the ASN-147 and GLU-146 residues are the most active residues in terms of bond distance and mostly repeated residue. Finally, among hydrogen and hydrophobic bonds, hydrophobic bonds showed weaker binding activity than hydrogen bonds in terms of bond distance.



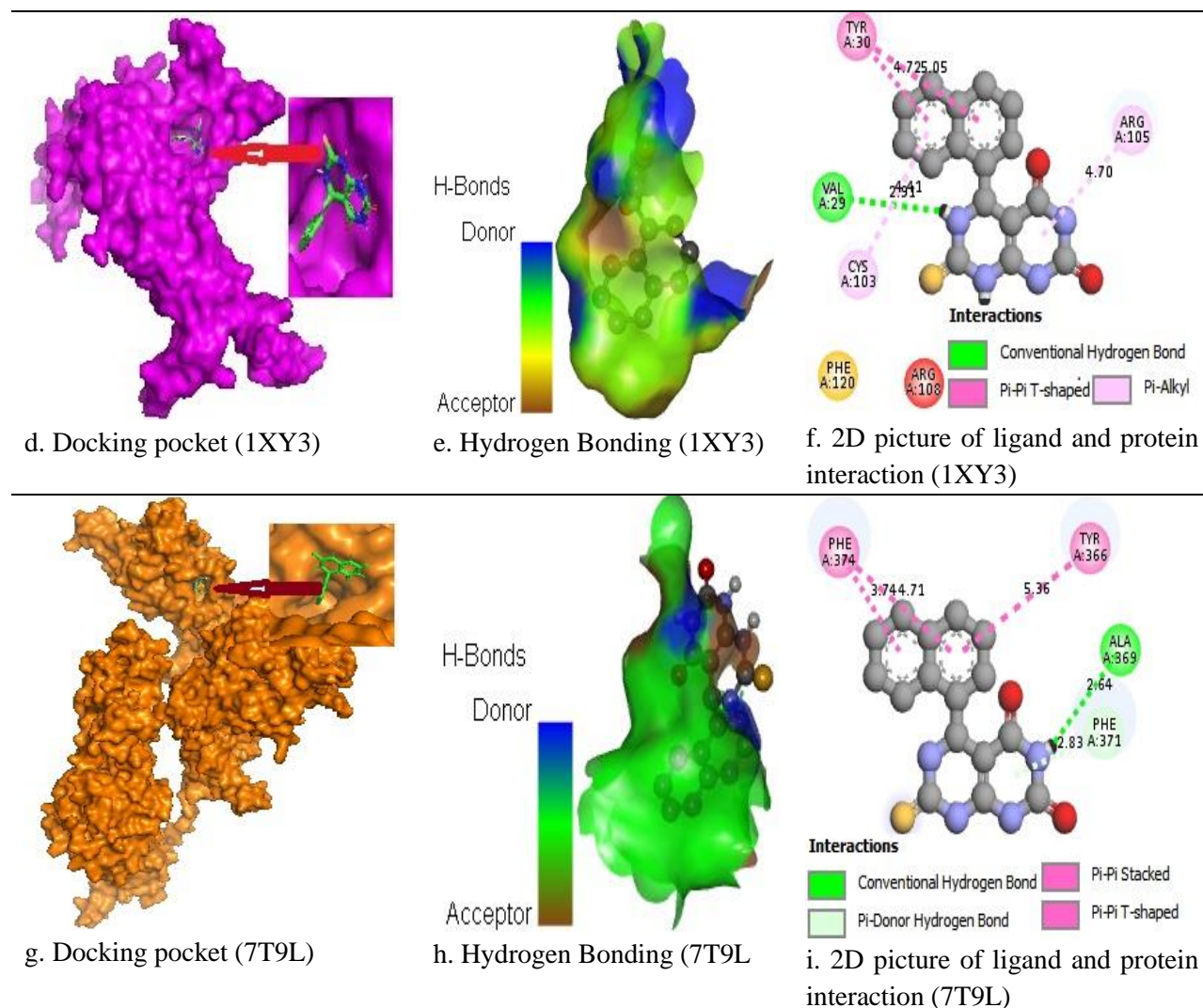


Figure 3. Protein ligands interaction of ligand PP1

For fungal protein, 1XY3, (*Aspergillus flavus*), GLU-259, TYR-30, and ARG-176 are the most repeatedly used amino acid residues by restating 6 times each. In addition, the lowest bond distance is at 1.933 Å with the residue ILE-177 for the ligand PP4. As shown in Table S2, amino acid residues, such as ILE-177, ARG-105, TRP-106, and GLU-259, have the other four lowest bond distances at 2.126 Å, 2.177 Å, 2.259 Å, and 2.342 Å, respectively in the ligands PP8, PP2, PP2, and PP4 respectively. It can be said that PP2 and PP4 have the strongest binding activity regarding their bond distance. Here, the residue with the lowest bond distance and the most repeated protein residues are totally different.

For omicron protein of 7T9L, VAL-124, ARG-243, and PHE-374 are the most repeated protein residues by repeating 5, 4 and 4 times, respectively, whereas PP7 has the lowest bond distance at 2.043 Å with the residue ASP-140. On the other hand, PP7, PP7, PP7, PP2 and PP3 have the lowest bond distance at 2.236 Å, 2.240 Å, 2.301 Å, and 2.321 Å with the residues, ARG-243, SER-244, SER-527, and TRP-433, respectively. Table S3 represents the protein ligand interaction with bond distance. Here, the PP7 has the highest number of lowest bond distances (three times) and most repeated residues have no lowest bond distances with ligands.

Figure 3 (a to i) clearly describes and shows how or where the protein and ligand are interacted. Also illustrated how the docking pocket, hydrogen bond and 2D structure of ligand PP1 are formed.

Antimicrobial activities of pyrimido[4,5-d]pyrimidine derivatives

3.8. Chemical Reactivity and Descriptors

The highest occupied molecular orbital is denoted by HOMO, whereas the lowest unoccupied molecular orbital is also expressed by LUMO. Both HOMO, and LUMO are considered significant for the orbitals of frontier molecular orbitals (FMO). Secondly, chemical reactivity increases when the energy gap between two levels narrows or becomes poor but chemical stability is similarly decreased. The energy, which conveys chemical reactivity, thermal stability, part of the electrophilic or nucleophilic attraction region, and biological dissociation or connection with protein, is listed in Table 8. Chemical reactivity, hardness, softness, part of the electrophilic or nucleophilic area, and biological dispersion or affiliation with protein, are all mentioned as energy.^{39,41,42} The energy difference between the HOMO and LUMO ranges from -6.00 to -9.00 eV, and is considered as the best-fitting for organic molecules.^{43,44}

Table 8. Frontier molecular orbitals and Reactivity descriptor analysis

Ligands	I=-HOMO	A=-LUMO	E GAP=I-A (eV)	Chemical potential: $(\mu) = -(I+A)/2$	Hardness: $(\eta) = (I-A)/2$	Softness $(\sigma) = 1/\mu$	Electronegativity: $(X) = (I+A)/2$	Electrophilicity $(\omega) = \mu^2/2\eta$
PP1	8.137	1.758	6.379	-4.948	3.190	0.314	4.948	3.837
PP2	8.669	1.811	6.858	-5.240	3.429	0.292	5.24	4.003
PP3	8.627	1.773	6.854	-5.200	3.427	0.292	5.200	3.945
PP4	8.627	1.820	6.807	-5.224	3.404	0.294	5.224	4.008
PP5	8.668	1.740	6.928	-5.204	3.464	0.289	5.204	3.909
PP6	8.794	1.774	7.020	-5.284	3.510	0.285	5.284	3.977
PP7	8.704	1.801	6.903	-5.253	3.452	0.290	5.253	3.996
PP8	8.996	1.818	7.178	-5.407	3.589	0.279	5.407	4.072
PP9	8.567	1.720	6.847	-5.144	3.424	0.292	5.144	3.863

The energy gaps of molecular orbitals are used to assess atomic electrical transportation properties. Good chemical stability depends on energy gaps. Good chemical stability is achieved when it has a broad HOMO-LUMO gap. If it has a narrow energy gap, then the compound will have a higher atomic system but lower chemical stability because HOMO-LUMO is close to each other. In this study, the e-gap ranges from 6.379 eV to 7.178 eV, which represents a broad E-gap that means those compounds have higher chemical stability and lower atomic system. However, the results differ expressively according to their functional group.^{45,46} Bioactivity can be described using the chemical potential (μ), hardness (h), softness (S), and electrophilicity coefficient.⁴⁷ Generally, softness should be lower than hardness. Absorption rate depends on the lower softness and hardness should be around 4.00 kcal/mol for good biological flexibility. In our study, all the pyrimido[4,5-d]pyrimidine derivatives are following the softness and hardness rule. Here, softness ranges from 0.290 to 0.314 and hardness ranges from 3.190 to 3.589, which are around the mentioned value. Chemical potentiality ranges from -4.948 eV to -5.407 eV which all are around the reference value of 5.00 eV. As a result, PP1 to PP9 are chemically potential. Table 08 depicts the frontier molecular orbitals and reactivity descriptors.

3.9. Frontier Molecular Orbitals of HOMO and LUMO

The HOMO and LUMO are the descriptors of chemical reactivity of molecules. Herein, the green color in LUMO denotes negative nodes, while the deep radish color denotes positive nodes. In the case of HOMO, the green and yellow is the indicator of positive and negative nodes of orbitals shown in Figure 4

and Figure S1 (Supplementary). The HOMO and LUMO are the active part of molecules by which they are attracted to the electrophilic and nucleophilic part of protein. As a result, the HOMO is the portion of bioactive compounds where the electrophilic attracting group may be introduced to generate chemical interaction, and the LUMO is the region of the positive part where the nucleophilic molecule may be added to create chemical interaction.⁴⁸⁻⁵¹ The LUMO part is located in the Pyrimidine ring of compounds and HOMO is found in the aromatic ring as the side chain in molecules. As it is the Pyrimidine derivatives so that this compound indicates the electrophilic nature.

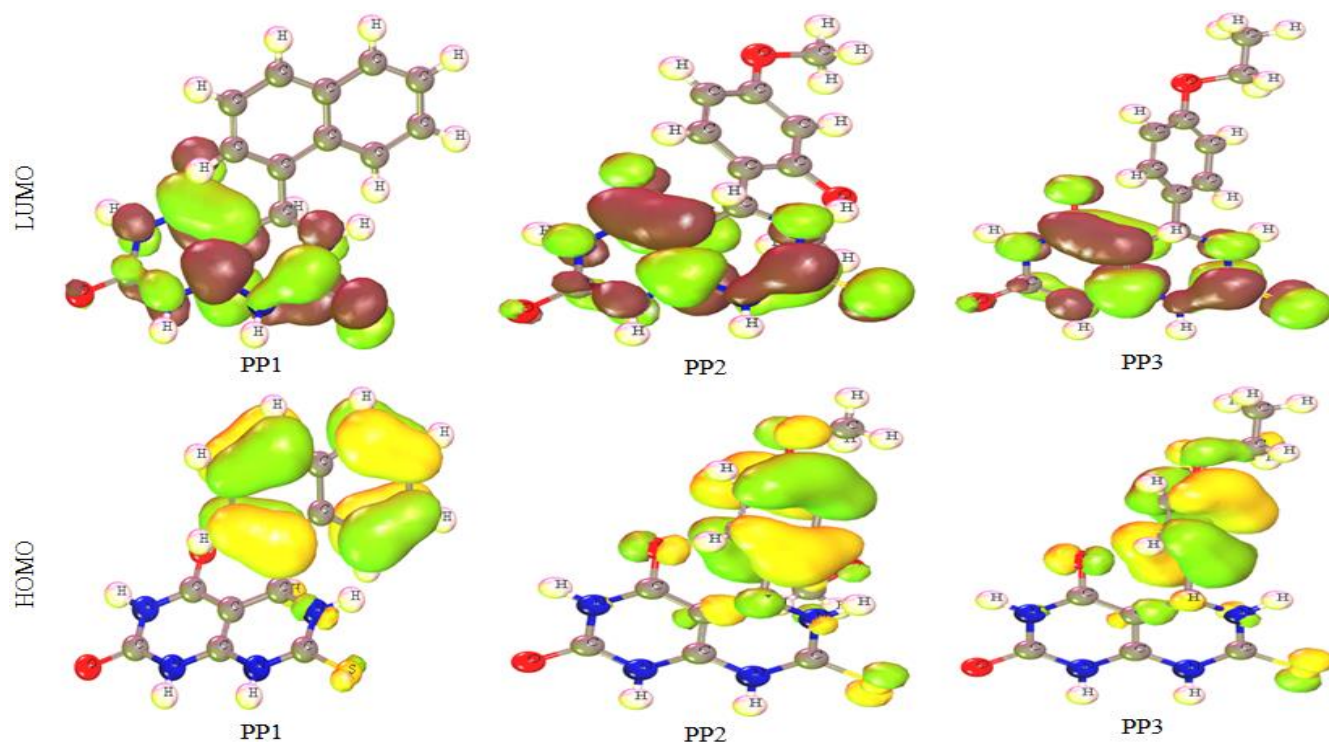


Figure 4. Frontier molecular orbital of HOMO and LUMO

3.10. Evaluation of Physicochemical and Drug Likeness Properties

The "Lipinski's rule of drug-likeness," often known as the "rule of five," is used to forecast the drug-like qualities of prospective compounds are depicted in Table 09. According to the criteria, if a molecule obeys at least four of the five qualities, it can be considered that this compound is following the Lipinski rule⁵² including Molecular weight ranges from 150 to 500 g/mol, five or fewer hydrogen bond donors, ten or fewer hydrogen bond acceptors, Csp3 hybridization more than 0.25, TPSA ranges from 20 to 130 Å², XLOGP3 will be between -0.7 and +5.0, log S not more than 6.⁵³ Here, the entire compound from PP1 to PP9 follow all the reference data of MW, number of hydrogen bond acceptors and donors, and fraction of Csp3. For TPSA, without PP6 and PP7, the rest of the compounds are in the accepted range. All (PP1-PP9) of the nine compounds are following all five rules of Lipinski and there is no violation either. PP1, PP3, PP5, PP8, and PP9 have high GI absorption and PP2, PP4, PP6 and PP7 have low GI absorption. All the nine compounds are showing good bioavailability as it is known that 0.55 is the indicator of good bioavailability.⁵⁴

Antimicrobial activities of pyrimido[4,5-d]pyrimidine derivatives

Table 9. Evaluation of physicochemical and Drug likeness properties

Legend Number	Molecular weight g/mol	Num. H-bond acceptors	Num. H-bond donors	Fraction Csp ³	TPSA (Å ²)	Log P _{ow} (XLOGP3)	Log S (ESOL)	Drug likeness (Lipinski Rules)		Bioavailability	GI absorption
								Follow	Violation		
PP1	324.36	2	4	1.00	127.55	2.62	-3.95	5	0	0.55	High
PP2	334.35	4	4	1.00	129.01	1.31	-2.93	5	0	0.55	Low
PP3	318.35	3	4	1.00	129.78	1.70	-3.09	5	0	0.55	High
PP4	318.44	3	4	1.00	126.78	1.34	-2.86	5	0	0.55	Low
PP5	288.32	2	4	1.00	120.55	1.73	-3.10	5	0	0.55	High
PP6	304.32	3	4	1.00	139.78	1.34	-2.86	5	0	0.55	Low
PP7	290.30	3	5	1.00	150.78	1.01	-2.65	5	0	0.55	Low
PP8	308.74	2	4	1.00	125.55	1.99	-3.39	5	0	0.55	High
PP9	288.32	2	4	1.00	120.55	1.73	-3.10	5	0	0.55	High

3.11. Pharmacokinetics Parameters and ADMET Properties Evaluation

Absorption, distribution, metabolism, excretion, and toxicity are the pharmacokinetics properties of a compound which is shortly known as ADMET. Those properties indicate the safety of a compound. Intestinal absorption needs to be >30% to be a highly absorbed molecule. If the value of log K_p > -2.5 then it has low skin permeability and >0.90 cm/s is considered high Caco2 permeability, which is not a violation of ADMET properties. Those with a logPS < -3 are thought to be unable to penetrate the CNS.⁵⁵⁻⁵⁷

Intestinal absorption is more than 60% which indicates a high absorption rate and skin permeability is low for all the compounds. Those compounds have no BBB permeability effect. Without PP5 and PP9, another seven compounds have lower logPS value than -3, so, those compounds are unable to penetrate the CNS. No compound can inhibit the CYP2C9 but PP6, PP7, and PP9 can inhibit the CYP1A2. Total clearance ranges from 0.647 to 0.884. Total clearance is lowest for PP7 and Highest for PP1. On the other hand, Renal OCT2 substrate excretions are done by PP2, PP5, PP7, and PP9, the rest of the compound cannot. PP1, PP3, PP4, PP6, and PP8 are not mutagenic but PP2, PP5, PP7, and PP9 are mutagenic. LD50 represents the toxicity level of a compound, in our study Toxicity level for all nine compounds are grade 4 (500 to 5000 mg/kg),⁵⁸ which represents the slightly toxic compound. Table 13 depicted the ADMET properties of pyrimido[4,5-d]pyrimidine derivatives.

The CYP1A3 substrate is responsible for the metabolism of drugs which is related to the pharmacokinetics of drugs and access to cytochrome P450 substrate. The PP1, PP2, PP3, PP4, PP5 and PP8 cannot inhibit the cytochrome but others can inhibit it. The AMES test is a widely employed method to assess a compound's mutagenic potential using bacteria. A positive test indicates that the compound is mutagenic and therefore may act as a carcinogen. Using this model, it is predicted the carcinogenic toxicity of study compounds. The compounds, PP1, PP3, PP4, PP6, and PP8 do not respond to the AMES toxicity, and PP2, PP5, PP7 and PP9 show the AMES toxicity. It is the Rat of lethal dosage values (LD50). It is the important factor of toxicity of a potential compound, and it is the amount of compound that causes the death of 50% of a group of tested animals in rats. The value of LD50 for PP1 to PP9 is about 2.119 to 2.690 mol/kg shown in Table 10.

Table 10. Pharmacokinetics parameters and ADMET properties evaluation

Ligand number	Absorption			Distribution			Metabolism		Excretion		Toxicity	
	Intestinal Absorption (% Absorbed)	Skin Permeability (log Kp)	Caco2 permeability (log Papp in 10-6 cm/s)	BBB permeability (log BB)	CNS permeability (log PS)	CYP2C9 inhibitor	CYP1A2 inhibitor	Total Clearance (log mL/min/kg)	Renal OCT2 substrate	AMES toxicity	LD50 (mol/kg)	
PP1	72.740	-2.735	-0.305	No	-3.541	No	No	0.884	Yes	No	2.317	
PP2	60.736	-2.735	0.048	No	-3.828	No	No	0.716	No	Yes	2.199	
PP3	65.389	-2.735	-0.022	No	-3.210	No	No	0.730	No	No	2.663	
PP4	64.626	-2.735	-0.011	No	-3.245	No	No	0.665	No	No	2.691	
PP5	66.328	-2.735	0.019	No	-2.925	No	No	0.662	No	Yes	2.582	
PP6	64.632	-2.735	-0.015	No	-3.202	No	Yes	0.683	No	No	2.649	
PP7	60.575	-2.735	-0.156	No	-3.183	No	Yes	0.647	Yes	Yes	2.471	
PP8	67.048	-2.735	-0.290	No	-3.653	No	No	0.748	No	No	2.284	
PP9	66.33	-2.735	-0.027	No	-2.919	No	Yes	0.662	Yes	Yes	2.590	

3.12. QSAR and pIC50 Studies

The following MLR equation is used for calculating pIC50 values.

Here, pIC50 (Activity) = $-2.768483965 + 0.133928895 \times (\text{Chiv5}) + 1.59986423 \times (\text{bcutm1}) + (-0.02309681) \times (\text{MRVSA9}) + (-0.002946101) \times (\text{MRVSA6}) + (0.00671218) \times (\text{PEOEVSAs}) + (-0.15963415) \times (\text{GATsv4}) + (0.207949857) \times (\text{J}) + (0.082568569) \times (\text{Diametert})$

A multiple linear regression equation is used to investigate the association between a single dependent variable (pIC50) and a set of independent variables (descriptors Chiv5, bcutm1, MRVSA9, MRVSA6, PEOEVSAs, GATsv4, J, and Diametert). Table 11 shows that the pIC50 ranges from 4.54 to 5.15, which represents the standard value of a compound.

Table 11. QSAR and pIC50

Ligand Number	PP1	PP2	PP3	PP4	PP5	PP6	PP7	PP8	PP9
PIC50	5.15	4.50	4.89	4.76	4.84	4.80	4.70	4.54	4.87

3.13. Molecular Electrostatic Potential (MEP) Charge Distribution

Molecular electrostatic potential is a useful tool for defining how the positive and negative charges (total charges) are distributed through the molecule. It can detect the presence of any suitable binding sites for ligands or proteins and can also determine the suitable attack site for nucleophilic or electrophilic sites of the compounds.⁵⁹ In Figure 5 below, the red color demonstrates the positive electrostatic potential region (electrophilic site), whereas the nucleophilic attack region is highlighted by the blue color. The negatively charged portion is observed to be larger than the positive charge zone. The Figure 5 and Figure S2 are demonstrating that the electrophilic sites within those compounds seem to be more desirable.

Antimicrobial activities of pyrimido[4,5-d]pyrimidine derivatives

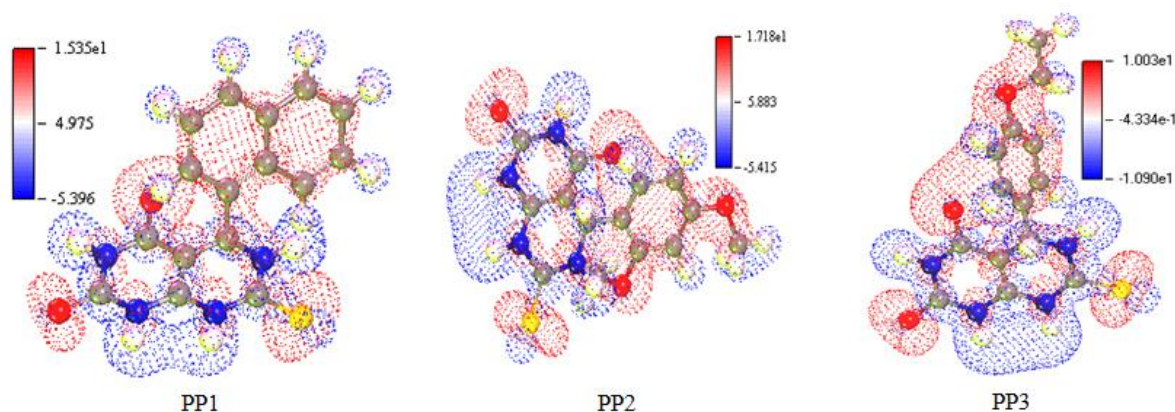


Figure 5. Map of Molecular Electrostatic Potential (MEP) charge distribution of the reported compounds

3.14. UV Visible Spectrum

UV-visible Spectroscopy is a great tool for determining the character of nitrogen ions with anion interaction.⁶⁰ pyrimido[4,5-d]pyrimidine derivatives have a maximum ranges of wavelength ranges from 246 nm to 377 nm.⁶¹ In this study, UV-visible spectroscopy shows the wavelength between 310 nm to 335 nm as shown in Figure S3, which confirms the compounds as pyrimido[4,5-d]pyrimidine derivatives.

3.15. Characterization by Electrostatic Vibrational Spectra (FTIR)

Vibrational spectroscopy can be used to determine the presence of a functional group in a compound. Almost all the experimental and calculated data of IR are the same, that is why it can be said that those compounds are validated as a pyrimido[4,5-d]pyrimidine derivatives. Figure S4 and Table 12 clearly demonstrate the IR value.

Table 12. Experimented and calculated IR values

Ligand Number	Experimental ⁴⁰	Calculated
PP1	3233, 3246, 1678,	3300, 1680
PP2	3211, 3373, 1678, 1562	2664, 2797, 1670
PP3	3360, 3375, 1678, 1560, 1180	2666, 2830, 1655
PP4	3366, 3375, 1680, 1570, 1160	2734, 1674
PP5	3345, 3377, 1678	2749, 1676
PP6	3300, 3390, 1680, 1180	2749, 1670
PP7	3290, 3360, 3390, 1685	3280, 3356, 1658
PP8	3350, 3380,	3311, 1676
PP9	3300-3350, 1682	2764, 1680

3.16. Molecular Dynamics Simulations

The root-mean-square deviation (RMSD) is a typical way to assess physical length. In other words, it indicates how much the protein shape has altered. The root mean square fluctuation, on the other hand, is a measurement to check how much a residue changes (fluctuates) at the time of a simulation. Molecular dynamics is a method for estimating the RMSD and RMSF of docking efficiency.⁶² To be a good fitting

pose of a drug pocket, the value of RMSD should be less than 2.0 Å and the ligand-protein complex must be able to dock properly by the program. It should be considered non-binder if RMSD values cross 2.0 Å and the complexes shall lose their stability.^{63,64}

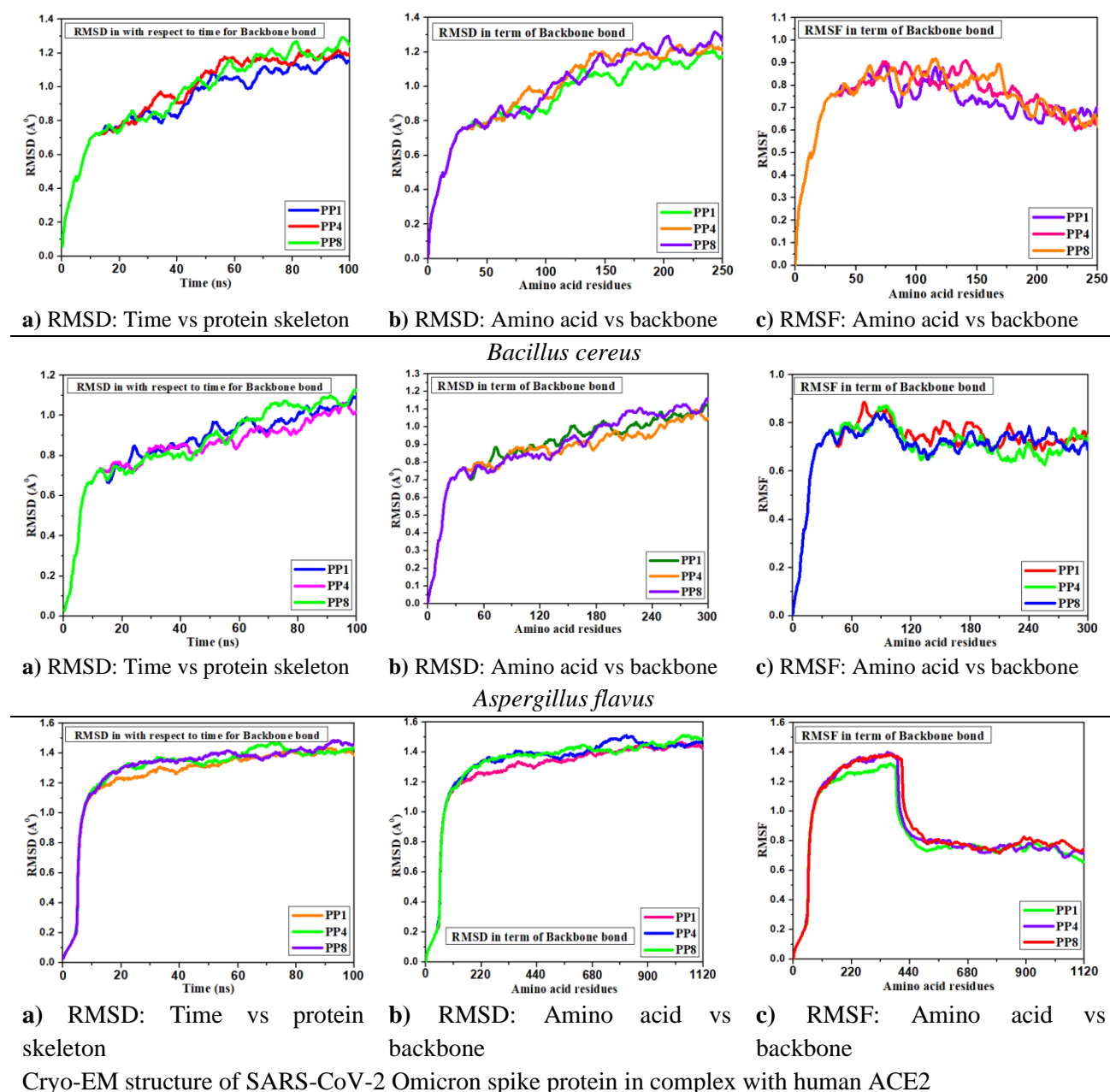


Figure 6. Molecular dynamics of the best three compounds

MD is performed against the complex of PP1, PP4 and PP8. According to the docking score, DFT, ADMET studies, these complexes are found to be the best compound against bacteria, fungus and omicron variants. The RMSD value of PP1, PP4 and PP8 complexes with bacterial protein 1AH7 is ranging from 1.1 Å to 1.3 Å in terms of time versus protein skeleton and RMSF value in terms of Amino acid versus backbone is lower than 0.7 Å and the trend is downward. Again, complexes with the fungal protein of *Aspergillus flavus* (1XY3) shows RMSD value lower than 1.2 Å and RMSF value is lower than 0.8 Å and it's also in a downward trend. At last, the RMSD values of the complexes with the omicron protein 7T9L are less than 1.6 Å and with the downward trend of RMSF value is lower than 0.8 Å. The RMSD value for time versus protein skeleton and Amino acid versus backbone are almost the same. For all the three

Antimicrobial activities of pyrimido[4,5-d]pyrimidine derivatives

compounds, there is a little bit of fluctuation that proves that all the compounds have almost the same effect against bacteria, fungus and omicron variant of COVID-19. Figure 6 indicates that PP1, PP4, and PP8 are highly potential and stable.

3.17. Antimicrobial Activities (In-Vitro)

Antibacterial activity of pyrimido[4,5-d]pyrimidine derivatives are examined in the Inorganic Research Laborator of Jahangirnagar University. In this study, the synthesized dihydropyrimidinones (Figure 1) were selected and screened for their antibacterial activity against five human bacteria among the synthesized compound viz. Inhibition by pyrimido[4,5-d]pyrimidine derivatives are lower at almost less than half for *Pseudomona aeruginosa*, *Escherichia coli*, *Shigella dysenteriae* and *Salmonella typhi* but inhibition against *Bacillus cereus* is higher than standard. Inhibition by standard is 11 µg (dw)/ disc whereas inhibition by PP1, PP4 and PP8 is 11.5, 11.1 and 11 µg (dw)/ disc respectively against *Bacillus cereus* bacteria. The compounds PP1, PP4 & PP8 were effective against *Bacillus cereus*. Overall, the result of tested chemical PP1 against *Bacillus cereus* was outstanding.

However, in the case of bacteria, PP4 has the highest docking score, which has a methoxy (-OCH₃) group in position number 3 of the benzene ring whereas in the case of PP6, it has the lowest docking score because of the same functional group with the highest distance. To sum up, after increasing the distance among functional groups with active compounds, docking scores start to decrease. Secondly, PP1 has the highest docking score where there is a double benzene ring with an active compound. PP3 has the lowest docking score and it has an ethoxy group. It is observed that the distance between functional groups is increased from the active compound, and consequently the docking score is decreased. In the case of omicron protease, the double benzene ring is found in ligand number PP4, which has the highest docking score. On the other hand, PP6 has a methoxy group in the 4th position of benzene, showing the lowest docking score, because of increasing the distance between the methoxy group and the main compound. This study must theoretically concluded that the distance is the cardinal fact for binding affinity among all pathogenic proteins not nature of specific functional groups in pyrimido[4,5-d]pyrimidine derivatives, and target docking score is always lower than auto docking score. Finally, the *in vitro* result gives give the similar supports to the *in silico* study.

Table 12. Diameter of Zone of inhibition in mm (100 µg (dw)/ disc) (*In Vitro*)

Bacteria	PP1	PP2	PP3	PP4	PP5	PP6	PP7	PP8	PP9	Control	Standard (ampicillin)
<i>Pseudomona aeruginosa</i>	6.5	6.0	6.9	5.9	5.5	7.0	8.2	5.8	8.3	0	20
<i>Escherichia coli</i>	7.7	5.8	6.5	6.1	6.2	6.0	6.2	6.0	6.3	0	12
<i>Bacillus cereus</i>	11.5*	6.0	7.0	11.1	8.3	6.9	6.5	11	6.7	0	11
<i>Shigella dysenteriae</i>	8.0	7.2	8.5	7.8	6.4	7.9	7.6	9.0	7.3	0	30
<i>Salmonella typhi</i>	5.8	5.5	5.9	6.2	6.0	6.1	6.1	6.5	6.2	0	24

4. Conclusions

Computer aided drug discovery tools on bacteria, fungus and omicron have been carried out by pyrimido[4,5-d]pyrimidine derivatives as inhibitors. To get a more accurate investigation, the both targeted and auto docking have been performed to calculate the binding affinity against bacteria, fungus, and omicron proteins. One standard drug for each docking (auto and targeted) is taken, and the docking score of auto docking is lower than the targeted docking by the same ligand and proteins. Next, the molecular dynamics has also been performed to check its stability with protein by accounting for the value of RMSD,

and RMSF. It shows a remarkable stability of each docked complex. Next, the electrostatic potential map is studied. In addition, these compounds show better pharmacokinetic properties, non-carcinogenicity, slight mutagenicity, water solubility, no BBB permeability, and no CNS permeability for most of the compounds. Finally, it can be stated that pyrimido[4,5-d]pyrimidine derivatives are showing good pharmaceutical or bioactive properties against bacteria, fungus, and omicron variant by detailed computational approaches: molecular docking, protein ligand interactions, ADMET, Carcinogenicity, Pharmacokinetics, DFT, HOMO-LUMO, IR, UV, MEP, and Molecular Dynamics. Based on this study, it is clearly observed that pyrimido[4,5-d]pyrimidine derivatives are highly potential drug candidates against *Bacillus cereus* bacteria, *Aspergillus flavus* fungus, and Omicron variant. Specially PP1, PP4, PP8 can be potential antibiotic (*Bacillus cereus*), anti-fungal (*Aspergillus flavus*), anti-viral (Omicron variant). The efficacy can be increased by the further modification of those proposed drugs.

Supporting Information

Supporting information accompanies this paper on <http://www.acgpubs.org/journal/organic-communications>

ORCID

Mahbub Alam: [0000-0001-8978-4160](https://orcid.org/0000-0001-8978-4160)

Md. Eleas Kobir: [0000-0002-0908-9633](https://orcid.org/0000-0002-0908-9633)

Ajoy Kumer: [0000-0001-5136-6166](https://orcid.org/0000-0001-5136-6166)

Unesco Chakma: [0000-0003-1711-7216](https://orcid.org/0000-0003-1711-7216)

Parul Akter: [0000-0002-8273-255X](https://orcid.org/0000-0002-8273-255X)

Md. Mosharef Hossain Bhuiyan: [0000-0003-4279-151X](https://orcid.org/0000-0003-4279-151X)

References

- [1] Zhen, X.; Stålsby Lundborg, C.; Sun, X.; Zhu, N.; Gu, S.; Dong, H. Economic burden of antibiotic resistance in China, a national level estimate for inpatients. *Antimicrob. Resist. Infect. Cont.* **2021**, *10*(5). doi: 10.1186/s13756-020-00872-w
- [2] Hendrickson, J.A.; Hu, C.; Aitken S.L.; Beyda, N. Antifungal resistance, a concerning trend for the present and future. *Curr. Infect. Dis. Rep.* **2019**, *21*(12), 47. doi: 10.1007/s11908-019-0702-9.
- [3] Menezes K.; De Oliveira-Smith P.J.; Woodworth AV. *Programming for Health and Wellbeing in Architecture*. Routledge London; UK, **2021**.
- [4] Venkatesh T.; Bodke Y.D.; S.J. AR. Facile CAN catalyzed one pot synthesis of novel indol-5; 8-pyrimido [4; 5-d] pyrimidine derivatives and their pharmacological study. *Chem Data Collect.* **2020**, *25*, 100335. doi:10.1016/j.cdc.2019.100335.
- [5] Aksinenko A.Y.; Goreva T.V.; Epishina T.A.; Trepalin S.V.; Sokolov V.B. Synthesis of bis (trifluoromethyl) pyrimido [4; 5-d] pyrimidine-2; 4-diones and evaluation of their antibacterial and antifungal activities. *J Fluor Chem.* **2016**, *188*, 191-195.
- [6] Srivastava S.K.; Haq W.; Chauhan P.M.S. Solid phase synthesis of structurally diverse pyrimido [4; 5-d] pyrimidines for the potential use in combinatorial chemistry. *Bioorg Med Chem Lett.* **1999**, *9*(7), 965-966.
- [7] Das S.; Thakur A.J.; Medhi T.; Das B. An efficient stereo-controlled synthesis of bis-pyrimido-[4; 5-d]-pyrimidine derivatives via aza-Diels–Alder methodology and their preliminary bioactivity. *RSC Adv.* **2013**, *3*(10), 3407-3413.
- [8] Brown D.J. Pyrimidines and their benzo derivatives. Published online **1984**.
- [9] Roth B.; Cheng C.C. 6 recent progress in the medicinal chemistry of 2; 4-diaminopyrimidines. *Prog Med Chem.* **1982**, *19*, 269-331.
- [10] Petrie III C.R.; Cottam H.B.; McKernan P.A.; Robins R.K.; Revankar G.R. Synthesis and biological activity of 6-azacadequomycin and certain 3; 4; 6-trisubstituted pyrazolo [3; 4-d] pyrimidine ribonucleosides. *J Med Chem.* **1985**, *28*(8), 1010-1016.
- [11] Bhuiyan M.H.; Rahman K.M.; Hossain K.; Rahim A.; Hossain M.I.; Naser M.A. Synthesis and antimicrobial evaluation of some new thienopyrimidine derivatives. *ACTA Pharm.* **2006**, *56*(4), 441-450.

Antimicrobial activities of pyrimido[4,5-d]pyrimidine derivatives

- [12] Abd El-aal El-Gaby M.S.; Abdel-Hamide S.G.; Ghorab M.M.; El-Sayed S.M. Synthesis and anticancer activity *in vitro* of some new pyrimidines. *Acta Pharm.* **1999**, *49*(3), 149-158.
- [13] Sondhi S.M.; Johar M.; Rajvanshi S.; Dastidar S.; Shukla R.; Raghbir R.; Lown J. Anticancer; anti-inflammatory and analgesic activity evaluation of heterocyclic compounds synthesized by the reaction of 4-isothiocyanato-4-methylpentan-2-one with substituted o-phenylenediamines; o-diaminopyridine and (un) substituted o. *Aust J Chem.* **2001**, *54*(1), 69-74. doi: 10.1071/CH00141.
- [14] Shishoo C.J.; Shirsath V.S.; Rathod I.S.; Patil M.J.; Bhargava S.S. Design; synthesis and antihistaminic (H1) activity of some condensed 2-(substituted) arylaminoethyl-pyrimidin-4 (3H)-ones. *Arzneimittelforschung.* **2001**, *51*(03), 221-231. doi: 10.1055/s-0031-1300028.
- [15] Nasr M.N.; Gineinah M.M. Pyrido [2; 3-d] pyrimidines and pyrimido [5'; 4', 5; 6] pyrido [2; 3-d] pyrimidines as new antiviral agents, synthesis and biological activity. *Arch. Pharm. (Int. J. Pharm. Med. Chem.)*. **2002**, *335*(6), 289-295.
- [16] Bruno O.; Brullo C.; Schenone S.; Ranise A.; Bondavalli F.; Barocelli E.; Tognolini M.; Magnanini F.; Ballabeni V. Progress in 5H [1] benzopyrano [4; 3-d] pyrimidin-5-amine series, 2-methoxy derivatives effective as antiplatelet agents with analgesic activity. *Il Farmaco* **2002**, *57*(9), 753-758.
- [17] Bhuiyan M.M.H.; Rahman K.M.M.; Hossain M.K.; Rahim M.A.; Hossain M.I. Fused pyrimidines. Part II, Synthesis and antimicrobial activity of some furo [3; 2-e] imidazo [1; 2-c] pyrimidines and furo [2; 3-d] pyrimidines. *Croat. Chem. acta.* **2005**, *78*(4), 633-636.
- [18] Bommegowda Y.D.; Shenoy D.B.; Menaka T.; Chethan B.P.; Nagaraja G.; Fazil Baig.; Sandeep K.N.; Babu V. Synthesis of novel pyrimido-[5; 4-d] pyrimidines by sequential nucleophilic substitution reaction. *J Chem. Pharm. Res.* **2012**, *4*(11), 4888-4893.
- [19] El-Moghazy S.M.; Ibrahim D.A.; Abdelgawad N.M.; Farag N.A.H.; El-Khouly A.S. Design; synthesis and biological evaluation of novel pyrimido [4; 5-d] pyrimidine CDK2 inhibitors as anti-tumor agents. *Sci. Pharm.* **2011**, *79*(3), 429-448.
- [20] Pasi M.; Tiberti M.; Arrigoni A.; Papaleo E. XPyder, A PyMOL plugin to analyze coupled residues and their networks in protein structures. *J. Chem. Inf. Model.* **2012**, *52*(7), 1865-1874.
- [21] Delley B. Time dependent density functional theory with DMol3. *J. Phys. Condens. Matter.* **2010**, *22*(38), 384208. doi: 10.1088/0953-8984/22/38/384208.
- [22] Methodologies C. The activity of alkyl groups in morpholinium cation on chemical reactivity; and biological properties of morpholinium tetrafluoroborate ionic liquid using the DFT method. *Chem. Methodol.* **2020**, *4*(2), 130-142.
- [23] Vijesh A.M.; Isloor A.M.; Telkar S.; Arulmoli T.; Fun H.K. Molecular docking studies of some new imidazole derivatives for antimicrobial properties. *Arab. J. Chem.* **2013**, *6*(2), 197-204.
- [24] D Studio, discovery studio life science modeling and simulations. *ResearchGateNet*. Published online **2008**, 1-8.
- [25] Nataraj A.; Balachandran V.; Karthick T. Molecular structure; vibrational spectra; first hyperpolarizability and HOMO-LUMO analysis of p-acetylbenzoxonitrile using quantum chemical calculation. *J. Mol. Struct.* **2013**, *1038*, 134-144.
- [26] Daina A.; Michielin O.; Zoete V. SwissADME, A free web tool to evaluate pharmacokinetics; drug-likeness and medicinal chemistry friendliness of small molecules. *Sci Rep.* **2017**, *7*, 1-13. doi: 10.1038/srep42717.
- [27] Mvondo J.G.M.; Matondo A.; Mawete D.T.; Bambi S.M.N.; Mbala B.M.; Lohohola P.O. *In Silico* ADME/T properties of quinine derivatives using SwissADME and pkCSM web servers. *Int. J. Trop. Dis. Heal.* **2021**, 1-12. doi: 10.9734/ijtdh/2021/v42i1130492.
- [28] Nisha C.M.; Kumar A.; Nair P.; Gupta N.; Silakari C.; Tripathi T.; Kumar a. Molecular docking and *in silico* admet study reveals acylguanidine 7a as a potential inhibitor of β -secretase. *Adv. Bioinformatics.* **2016**. doi: 10.1155/2016/9258578.
- [29] Ayers P.W.; Parr R.G. Variational principles for describing chemical reactions, The Fukui function and chemical hardness revisited. *J. Am. Chem. Soc.* **2000**, *122*(9), 2010-2018.
- [30] Kohn W.; Becke A.D.; Parr R.G. Density functional theory of electronic structure. *J. Phys. Chem.* **1996**, *100*(31), 12974-12980.
- [31] Parr R.G.; Szentpály L.V.; Liu S. Electrophilicity index. *J. Am. Chem. Soc.* **1999**, *121*(9), 1922-1924.
- [32] Komanduri R.; Raff L.M. A review on the molecular dynamics simulation of machining at the atomic scale. *Proc. Inst. Mech. Eng. Part B J. Eng. Manuf.* **2001**, *215*(12), 1639-1672.
- [33] Dong J.; Cao D.S.; Miao H.Y.; Liu S.; Deng B.C.; Yun Y.H.; Wang N.N.; Lu A.P.; Zeng W.B.; Chen A.F. ChemDes, An integrated web-based platform for molecular descriptor and fingerprint computation. *J. Cheminform.* **2015**, *7*(1), 1-10. doi: 10.1186/s13321-015-0109-z.
- [34] Verma J.; Khedkar V.; Coutinho E. 3D-QSAR in drug design - A Review. *Curr Top Med Chem.* **2010**, *10*(1), 95-115.

- [35] Peter S.C.; Dhanjal J.K.; Malik V. Quantitative structure-activity relationship (QSAR), modeling approaches to biological applications. In: Encyclopedia of Bioinformatics and Computational Biology, *Elsevier Ltd.*, **2018**, 1-3(1964), 661-676. Doi:10.1016/b978-0-12-809633-8.20197-0
- [36] Biemer J.J. Antimicrobial susceptibility testing by the Kirby-Bauer disc diffusion method. *Ann. Clin. Lab. Sci.* **1973**, 3(2), 135-140.
- [37] Bhuiyan M.H.; Matin M.M. Derivatives reactions, synthesis and of pyrimido [4 ;5-d] pyrimidine. **2014**, 28-36.
- [38] Kumer A.; Khan M.W. Synthesis; characterization; antimicrobial activity and computational exploration of ortho toluinium carboxylate ionic liquids. *J. Mol. Struct.* **2021**, 1245. doi:10.1016/j.molstruc.2021.131087.
- [39] Kumer A.; Khan M.W. The effect of alkyl chain and electronegative atoms in anion on biological activity of anilinium carboxylate bioactive ionic liquids and computational approaches by DFT functional and molecular docking. *Heliyon* **2021**, 7(7). doi: 10.1016/j.heliyon.2021.e07509.
- [40] Nath A.; Kumer A.; Khan M.W. Synthesis; computational and molecular docking study of some 2; 3-dihydrobenzofuran and its derivatives. *J. Mol. Struct.* **2021**, 1224. doi: 10.1016/j.molstruc.2020.129225.
- [41] Nath A.; Kumer A.; Zaben F.; Khan M.W. Investigating the binding affinity; molecular dynamics; and ADMET properties of 2; 3-dihydrobenzofuran derivatives as an inhibitor of fungi; bacteria; and virus protein. *Beni-Suef Univ. J. Basic. Appl. Sci.* **2021**, 10(1), 1-13.
- [42] Hoque MM; Hussien MS; Khan MW. Theoretical Evaluation of 5; 6-Diaroylisoindoline-1;3-dione as Potential Carcinogenic Kinase PAK1 Inhibitor, DFT Calculation; Molecular Docking Study and ADMET Prediction. *Int J Adv Biol Biomed Res.* **2021**, 9(1), 77-104. doi:10.1186/s43088-021-00117-8.
- [43] Hoque M.M.; Hussien M.S.; Kumer A.; Khan M.W. Synthesis of 5; 6-diaroylisoindoline-1; 3-dione and computational approaches for investigation on structural and mechanistic insights by DFT. *Mol Simul.* **2020**, 46 (16), 1298-1307.
- [44] Kumer, A. , Jahidul, M. I.; Paul, S.; Effect of External Electric Field and Temperature on Entropy, Heat of Capacity, and Chemical Reactivity with QSAR Study of Morphonium Chloride and Nitrous Ionic Liquids Crystal Using DFT. *Chem. Methodol.* **2020**, 4(5): 595-604; DOI-510.22034/CHEMM.2020.107203.
- [45] Parr R.G.; Szentpály L.v; Liu S. Electrophilicity index. *J. Am. Chem. Soc.* **1999**, 121(9), 1922-1924.
- [46] Ahmed M.K.; Kumer A.; Imran A. Bin. Facile fabrication of polymer network using click chemistry and their computational study. *R Soc Open Sci.* **2021**, 8(3). doi: 10.1098/rsos.202056
- [47] Kumer A.; Paul S.; Sarker M.N.; Islam M.J. The prediction of thermo physical; vibrational spectroscopy; chemical reactivity; biological properties of morpholinium borate; phosphate; chloride and bromide Ionic Liquid, A DFT Study. *Int. J. New. Chem.* **2019**, 6(4), 236-253.
- [48] Kumer A.; Sarker M.N.; Paul S. The theoretical investigation of HOMO; LUMO; thermophysical properties and QSAR study of some aromatic carboxylic acids using HyperChem programming. *Int. J. Chem. Technol.* **2019**, 3(1), 26-37.
- [49] Islam M.J.; Sarker N.; Kumer A. The evaluation and comparison of thermo-physical; chemical and biological properties of palladium (II) complexes on binuclear diamine ligands with different anions using the DFT method. *Int. J. Adv. Biol. Biomed. Res.* **2019**, 7(4), 315-334.
- [50] Zhang M.Q.; Wilkinson B. Drug discovery beyond the “rule-of-five.” *Curr. Opin. Biotechnol.* **2007**, 18(6), 478-488.
- [51] Daina A.; Michielin O.; Zoete V. SwissADME, A free web tool to evaluate pharmacokinetics; drug-likeness and medicinal chemistry friendliness of small molecules. *Sci. Rep.* **2017**, 7, 1-13. doi: 10.1038/srep42717.
- [52] Martin Y.C. A bioavailability score. *J. Med. Chem.* **2005**, 48(9), 3164-3170.
- [53] Pires D.E.V.; Blundell T.L.; Ascher D.B. pkCSM, Predicting small-molecule pharmacokinetic and toxicity properties using graph-based signatures. *J. Med. Chem.* **2015**, 58(9), 4066-4072.
- [54] Vogel K.E. Chapter 14 Chapter 14. *LR Lloyd's Regist.* **2000**, 100, 1-35.
- [55] Cheng F.; Li, W.; Yadi, Z.; Shen J., Wu,Z.; Liu, G.; Philip, W. L.; and Tang, Y.; admetSAR: A Comprehensive Source and Free Tool for Assessment of Chemical ADMET Properties;. *Chem. Inf. Model.* **2012**, 52, 11, 3099–3105. <https://doi.org/10.1021/ci300367a>.
- [56] What is a LD50 and LC50? , OSH Answers. Accessed February 12, **2022**.
- [57] Tasi G.; Palink I.; Nyerges N. PA1 Fejes and HF. calculation of electrostatic potential maps and atomic charges for large molecules. **1993**, 33(3), 296-299.
- [58] Howard A.; McIver J.; Collins J. Hyperchem computational chemistry. *Hypercube Inc; Waterloo.* **1994**.
- [59] Cahyana A.H.; Liandi A.R.; Zaky M.Z.R. Efficiency and potential synthesis of pyrimido [4;5-d] pyrimidine derivatives by iodine catalyst as antioxidant agent. *IOP Conf. Ser. Mater. Sci. Eng.* **2020**, 902(1). doi:10.1088/1757-899X/902/1/012039
- [60] Allouche A. software news and updates gabedit — a graphical user interface for computational chemistry softwares. *J. Comput. Chem.* **2012**, 32, 174-182.

Antimicrobial activities of pyrimido[4,5-d]pyrimidine derivatives

- [61] Akash S.; Chakma U.; Chandro A.; Matin M.M.; Howlader D. The computational screening of inhibitor for black fungus and white fungus by D-glucofuranose derivatives using *in silico* and SAR study. *Org. Commun.* **2021**, *14* (4), 336-353.
- [62] Hashem H.E.; Nath A.; Kumer A. Synthesis; molecular docking; molecular dynamic; quantum calculation; and antibacterial activity of new Schiff base-metal complexes. *J. Mol. Struct.* **2022**, *1250*. doi: 10.1016/j.molstruc.2021.131915.

A C G
publications

© 2022 ACG Publications